J Incl Phenom Macrocycl Chem (2009) 63:131–139
DOI 10.1007/s10847-008-9497-2

ORIGINAL ARTICLE

Metal ion complexation in acetonitrile by di-ionized calix[4]arenes bearing two dansyl fluorophores

Ümmühan Ocak · Miraç Ocak · Kazimierz Surowiec · Richard A. Bartsch · Maryna G. Gorbunova · Chuqiao Tu · Malgorzata A. Surowiec

Received: 4 June 2008 / Accepted: 21 August 2008 / Published online: 9 September 2008

Abstract The influence of metal cations (Li^+, Na^+, K^+, Rb^+, Cs^+, Mg^{2+}, Ca^{2+}, Sr^{2+}, Ba^{2+}, Ag^+, Cd^{2+}, Co^{2+}, Fe^{2+}, Hg^{2+}, Mn^{2+}, Pb^{2+}, Zn^{2+} and Fe^{3+}) on the spectroscopic properties of two dansyl (1-dimethylaminonaphthalene-5-sulfonyl) groups linked to the lower rims of a series of three, structurally related, di-ionized calix[4]arenes was investigated by means of absorption and emission spectrophotometry. Di(tetramethylammonium) salts of the di-ionized ligands, $(TMA)_2L1$, $(TMA)_2L2$ and $(TMA)_2L3$, which differ in having zero, two and four *tert*-butyl groups, respectively, on the upper rim of the calix[4]arene scaffold were utilized for the spectrofluorimetric titration experiments in acetonitrile. On complexation by alkaline earth metal cations, both the absorption and emission spectra undergo marked red shifts and quenching of the dansyl fluorescence. These effects are weaker with alkali metal cations. Transition metal cations interact strongly with the ligands. In particular, Fe^{3+}, Hg^{2+} and Pb^{2+} cause greater than 97% quenching of the dansyl fluorescence in the di-ionized ligands.

Keywords Calixarene ligand · Fluorescence spectroscopy · Stability constant · Metal ion complexation

Ü. Ocak · M. Ocak · K. Surowiec · R. A. Bartsch · M. G. Gorbunova · C. Tu · M. A. Surowiec
Department of Chemistry and Biochemistry, Texas Tech University, Lubbock, TX 79409, USA

Ü. Ocak (✉) · M. Ocak
Department of Chemistry, Faculty of Arts and Sciences, Karadeniz Technical University, 61080 Trabzon, Turkey
e-mail: uocak@ktu.edu.tr

Introduction

Calix[n]arenes are an important class of synthetic macrocyclic ligands for complexation of cations [1–6]. Substituted calix[4]arenes are capable of binding alkali metal cations on the lower rim. In the bucket-shaped cone conformation, a three-dimensional scaffold provides sites for attaching various ligating groups to the lower rim. Ester functions have frequently been appended as lower-rim ligating groups. Also, it is possible to create polytopic ligands with binding sites on the upper rim. The cation binding properties of calix[4]arenes depend on the nature of cation and the substitution on the upper and/or lower rims.

Calixarenes substituted on the upper or lower rim may show selective cation recognition dependent on the cation-ligating group. This group, known as the ionophore, may be a crown ether, carboxylic acid, amide and other functional group. Recently, the cation–ionophore interaction has been monitored by a signaling moiety attached to the calixarene framework. The signaling moiety may be a fluorogenic unit, such as a pyrene, anthracene, naphthalene or dansyl group [7]. Functionalized calixarenes incorporating such fluorophores are known as fluorescent chemosensors, especially for cations.

In the last few years, a variety of chemosensors based on calix[4]arenes bearing fluorescent groups have been synthesized for investigation of their fluorescent responses upon complexation with various metal cations [7–10]. Recently, there has been strong interest in dansyl derivatives as potential fluorophores [11–16].

In 1999, Bartsch and coworkers reported the synthesis of substituted calix[4]arene **3** (Scheme 1) with two methoxy groups and two *N*-dansyl oxyacetamide functions on the lower rim and its use in selective sensing of Hg^{2+} by extraction from acidic aqueous solutions into chloroform [15]. Subsequently, Valuer and coworkers reported a

detailed study of the photophysical and complexing properties of ligand **3** in aqueous acetonitrile in which high selectivity for Hg^{2+} over interfering metal ions (Na^+, K^+, Ca^{2+}, Cd^{2+}, Cu^{2+}, Pb^{2+} and Zn^{2+}) and sensitivity in the 10^{-7} mol L^{-1} concentration range were observed [17]. Covalent attachment of a structurally related calix[4]arene bearing two *N*-dansyl oxyacetamide fluorophores to silica gel was performed and evaluated for optical sensing of Hg^{2+} in water [18]. The functionalized material was able to reversibly detect Hg^{2+} with a response time of a few seconds and a detection limit of 3.3×10^{-7} mol L^{-1} in water. The system showed high selectivity for Hg^{2+} over Na^+, K^+, Ca^{2+}, Cd^{2+}, Cu^{2+} and Pb^{2+}.

In this paper, we report the synthesis of calix[4]arene ligands **1** and **2** (Scheme 1). The structures of ligands **1–3** differ in having zero, two and four *tert*-butyl groups attached to the upper rim of the calix[4]arene scaffold. Responses of di(tetramethylammonium) salts of the di-ionizable ligands **1–3** to a variety of metal cations are assessed by spectrofluorometric titrations in acetonitrile. The complex stability constants and complex compositions of Hg^{2+}, Pb^{2+} and Fe^{3+} with the three ionized ligands are determined.

Experimental

Chemicals

Acetonitrile from EM (spectrometric grade) was utilized as the solvent for the absorption and fluorescence measurements. Alkali metal and earth alkaline metal perchlorates from Acros were of the highest quality available and were vacuum dried over silica gel before use. Other metal perchlorates were available from previous studies.

Apparatus

^1H NMR spectra were measured in $CDCl_3$ at 500 MHz with a Varian Unity INOVA spectrometer. IR spectra were recorded with a Perkin–Elmer model 1600 FT–IR spectrophotometer. Absorption spectra were recorded on a Shimadzu model 2401PC UV–visible spectrophotometer. Fluorescence spectra were obtained on a SLM Aminco 8000C photon counting spectrofluorometer equipped with a 450-W ozone-free xenon lamp as the light source. Combustion analysis was performed by Desert Analytics Laboratory in Tucson, Arizona.

Absorption and fluorescence measurements

Absorption spectra of the di-ionized ligands (2.58×10^{-5} M) in acetonitrile solutions containing 50 molar equivalents of appropriate metal perchlorate salt were measured using a 1 cm absorption cell. Fluorescence spectra of the same solutions were measured with a 1 cm quartz cell. The excitation wavelength was 326 nm for $(TMA)_2L1$ and $(TMA)_2L2$. The excitation wavelength was 328 nm for $(TMA)_2L3$. Fluorescence emission spectra were recorded in the range 400–750 nm with a slit width of 1.0 nm.

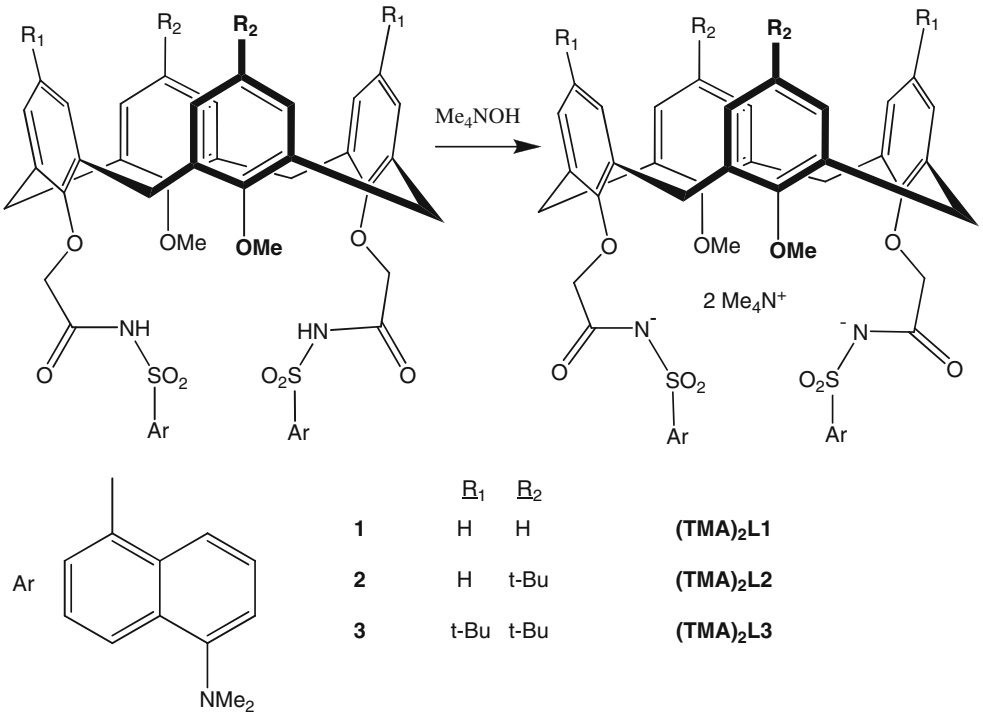

Scheme 1 Structures of ionophores **1–3** and their ionized tetramethylammonium salts $(TMA)_2L1$, $(TMA)_2L2$ and $(TMA)_2L3$, respectively

The stoichiometries of the complexes and their stability constants were determined according to a literature procedure [19].

Ligand synthesis

*25,27-Bis(N-(5-dimethylaminonaphthalene-1-sulfonyl)carbamoylmethoxy)-26,28-dimethoxycalix[4]arene (**1**)*

The precursor di(acid chloride) was prepared by a literature method [20]. To a mixture of sodium hydride (0.12 g, 5.0 mmol) and dansylamide (0.38 g, 1.5 mmol) in dry THF (10 ml) under nitrogen was added a solution of the di(acid chloride) (0.30 g, 0.50 mmol) in dry THF (20 ml). The mixture was stirred at room temperature for 12 h and then cooled in an ice-bath. Water was carefully added to destroy the excess of sodium hydride and the THF was evaporated in vacuo. Water was added to the residue and the aqueous mixture was extracted with dichloromethane. The organic extract was washed with water and dried over magnesium sulfate. After evaporation of the dichloromethane in vacuo, the crude product was purified by chromatography on silica gel with hexanes-ethyl acetate (1:4) as eluent. The residue was dissolved in dichloromethane, washed with 10% hydrochloric acid then water, dried over magnesium sulfate and evaporated in vacuo to give 0.35 g (67%) of **1** as a yellow solid with melting point of 167–172 °C. ^{1}H NMR (500 MHz, $CDCl_3$): δ 2.89 (s, 12H); 3.04–3.67 (m, 14H); 4.10–4.24 (m, 4H); 6.24–6.71 (m, 4H); 6.73–7.22 (m, 10H); 7.61–7.78 (m, 4H); 8.46–8.65 (m, 6H); 9.76, 9.50 (s, 2H). IR (deposit from dichloromethane solution on a sodium chloride plate): 1735 (C=O) cm^{-1}. Anal. Calcd. for $C_{58}H_{56}N_4O_{10}S_2$: C 67.42, H 5.46, N 5.42. Found: C 67.25, H 5.79, N 5.62%.

*5,17-Bis(1,1-dimethylethyl)-25,27-bis(N-(5-dimethylaminonaphthalene-1-sulfonyl)-carbamoylmethoxy)-26,28-dimethoxycalix[4]arene (**2**)*

The precursor di(acid chloride) was prepared by a literature method [20]. To a mixture of sodium hydride (0.52 g, 21.6 mmol) and dansylamide (1.36 g, 5.43 mmol) in THF (40 mL) under nitrogen was added a solution of the di(acid chloride) (1.30 g, 1.81 mmol) in THF (40 mL) and the mixture was stirred at room temperature for 12 h. After careful addition of water, the THF was evaporated in vacuo. To the residue, dichloromethane was added and the mixture was washed with 10% aqueous potassium carbonate. The organic layer was separated, dried over magnesium sulfate and evaporated in vacuo. The residue was chromatographed on silica gel with methanol-dichloromethane (1:20) as eluent. After partial evaporation of the eluent, the solution was washed with 10% hydrochloric acid and then with water (2 × 100 mL) and dried over magnesium sulfate. Evaporation in vacuo gave 0.60 g (52%) of **2** as a yellow solid with melting point of 220–222 °C. ^{1}H NMR (500 MHz, $CDCl_3$): δ 1.38 (br s, 18H); 3.04 (br s, 12H); 3.20 and 3.22 (overlapped br s, 4H); 4.15 and 4.21 (overlapped br s, 14H); 6.13 (br s, 2H), 6.32 (br s, 2H); 7.15 (s, 4H); 7.36 (br s, 2H); 7.74 (br s, 4H); 8.69, 8.70 (overlapped br s, 4H); 8.93 (br s, 2H); 9.76 (br s, 2H). IR (deposit from dichloromethane solution on a sodium chloride plate): 1737 (C=O) cm^{-1}. Anal. Calcd. for $C_{66}H_{72}N_4O_{10}S_2$: C, 69.25; H, 6.35; N, 4.89. Found: C, 68.88; H, 6.27; N, 4.81.

*5,11,17,23-Tetrakis(1,1-dimethylethyl)-25,27-bis (N-(5-dimethylaminonaphthalene-1-sulfonyl)carbamoylmethoxy)-26-28-dimethoxycalix[4]arene (**3**)*

This ligand was prepared according to the published procedure [15].

General procedure for preparation of the di(tetramethylammonium) salts of the di-ionized ligands

The ligand was dissolved in benzene. The benzene solution was vortexed with an excess of aqueous tetramethylammonium hydroxide (TMAOH) and the mixture was centrifuged. The benzene layer was separated and the benzene was evaporated in vacuo, which removed the residual water in the benzene layer. The resultant solid was the di(tetramethylammonium) salt of the di-ionized ligand.

Results and discussion

New didansyl di-ionizable ligands **1** and **2** were prepared and characterized by ^{1}H NMR spectroscopy and combustion analysis. Unlike the ^{1}H NMR spectrum of **3**, which was consistent with the cone conformation, the ^{1}H NMR spectra of **1** and **2** were much more complex, indicating that the ligands are conformationally mobile in $CDCl_3$. As judged from their ^{1}H NMR spectra, conformational mobility of the ligands decreases as *tert*-butyl groups are added to the upper rim. Ligands **1**–**3** were converted into their tetramethylammonium salts, $(TMA)_2L1$, $(TMA)_2L2$ and $(TMA)_2L3$, respectively, by reaction with tetramethylammonium hydroxide (Scheme 1). The di-ionized forms of the ligands with non-coordinating tetramethylammonium cations were used for the investigation of interactions with metal ion perchlorates in acetonitrile. Ligands **1–3** and ionized forms $(TMA)_2L1$, $(TMA)_2L2$ and $(TMA)_2L3$ differ in having zero, two and four *tert*-butyl groups on their upper rims, respectively. This type of structural variation

has been shown to influence both the efficiency and selectivity of competitive alkali metal cation extraction and competitive alkaline earth metal cation extraction from aqueous solutions into chloroform [20].

Absorption spectra

In acetonitrile, $(TMA)_2L1$ and $(TMA)_2L2$ exhibit a single absorption band with a maximum at 326 nm. $(TMA)_2L3$ shows an absorption band with a maximum at 328 nm. Molar absorption coefficients are 6.2×10^3, 4.7×10^3 and 6.0×10^3 cm^{-1} M^{-1} for ionized ligands $(TMA)_2L1$, $(TMA)_2L2$ and $(TMA)_2L3$, respectively, at these wavelength maxima. $(TMA)_2L2$, with two *tert*-butyl groups on the upper rim, has an additional absorption maximum at ~252 nm (Fig. 1a).

The presence of 50 equivalents of alkali or alkaline earth metal cations produces modest enhancements in the absorption of $(TMA)_2L1$ below 250 nm (Fig. 2a). Similar changes can be seen for $(TMA)_2L3$ (Fig. 2c). However the effect of these metal ions on the absorption spectra of $(TMA)_2L2$ are different (Fig. 2b). The absorption enhancements in the presence of alkaline and earth alkaline metal cations are smaller, except for K^+.

A majority of the transition metal cations investigated and Pb^{2+} cause large changes in the molar absorption coefficients of the short wavelength absorption band in the spectrum of $(TMA)_2L2$ (Fig. 1a). The molar absorption coefficient for the maximum at 252 nm increases by 29 and 21% in the case of Cd^{2+} and Pb^{2+}, respectively. The increment is 41% in case of Fe^{2+}. However, Hg^{2+} causes a decrease of 71% in the molar absorption coefficient of the 252 nm absorption. The long-wave absorption band (326 nm) is less sensitive to the presence of these cations, except for Pb^{2+} and Hg^{2+}. It is interesting that the interaction of Fe^{3+} (Fig. 1c) with $(TMA)_2L2$ markedly increases absorptions in all parts of the spectrum, particularly in the long wavelength band.

Table 1 shows changes in the absorption spectra of $(TMA)_2L1$, $(TMA)_2L2$ and $(TMA)_2L3$ in acetonitrile for the metal ions investigated. As can be seen from the data in Table 1, the alkali and earth alkaline metal cations shift the 326 and 328 nm absorption bands to the longer wavelengths. Li^+, Na^+, K^+, Rb^+ and Cs^+ produce 5 nm red shifts with $(TMA)_2L1$, while the same ions produce 3 nm red shifts with $(TMA)_2L3$. However $(TMA)_2L2$ shows 8 and 6 nm red shifts in the presence of Li^+ and Na^+, respectively. The red shifts for K^+, Rb^+ and Cs^+ are 5 nm. These red shifts can be explained as resulting from photoinduced charge transfer. The dansyl fluorophore includes an electron-donating group (dimethylamine) conjugated to an electron-withdrawing unit (carbonyl group). The electron-donating character of dimethylamine group increases upon interaction of a cation with the carbonyl group.

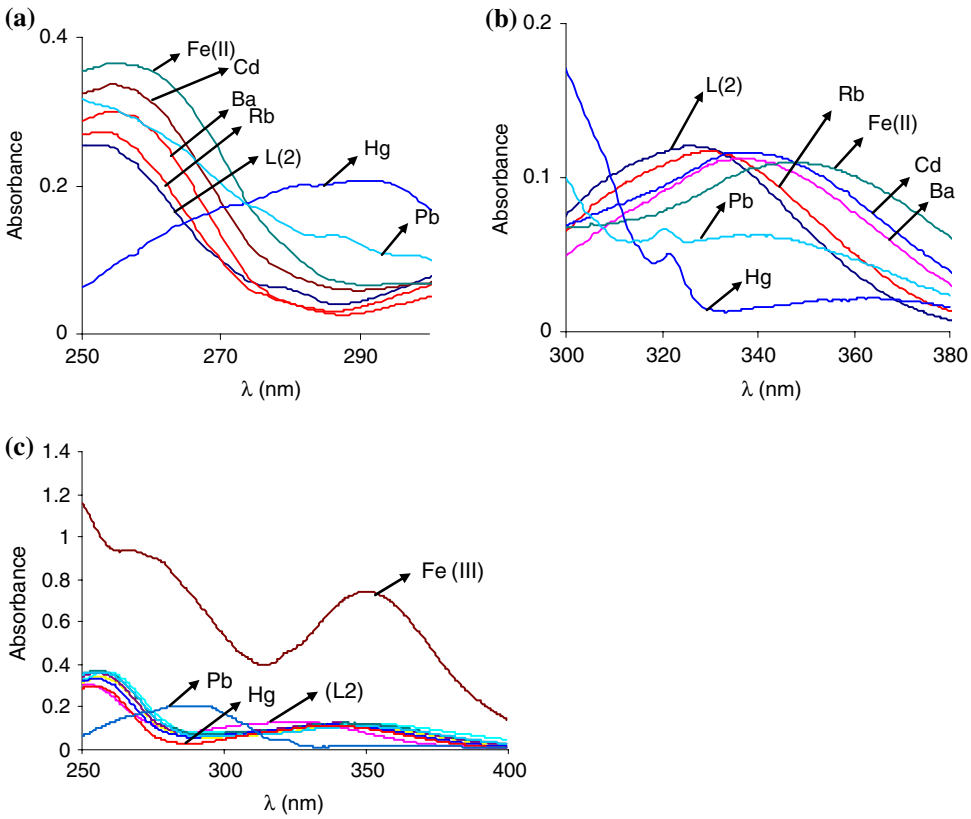

Fig. 1 Absorption spectra of $(TMA)_2L2$ (identified as L(2) and its complexes with metal cations in acetonitrile: (**a**) between 250 and 300 nm; (**b**) between 300 and 380 nm; and (**c**) between 250 and 400 nm

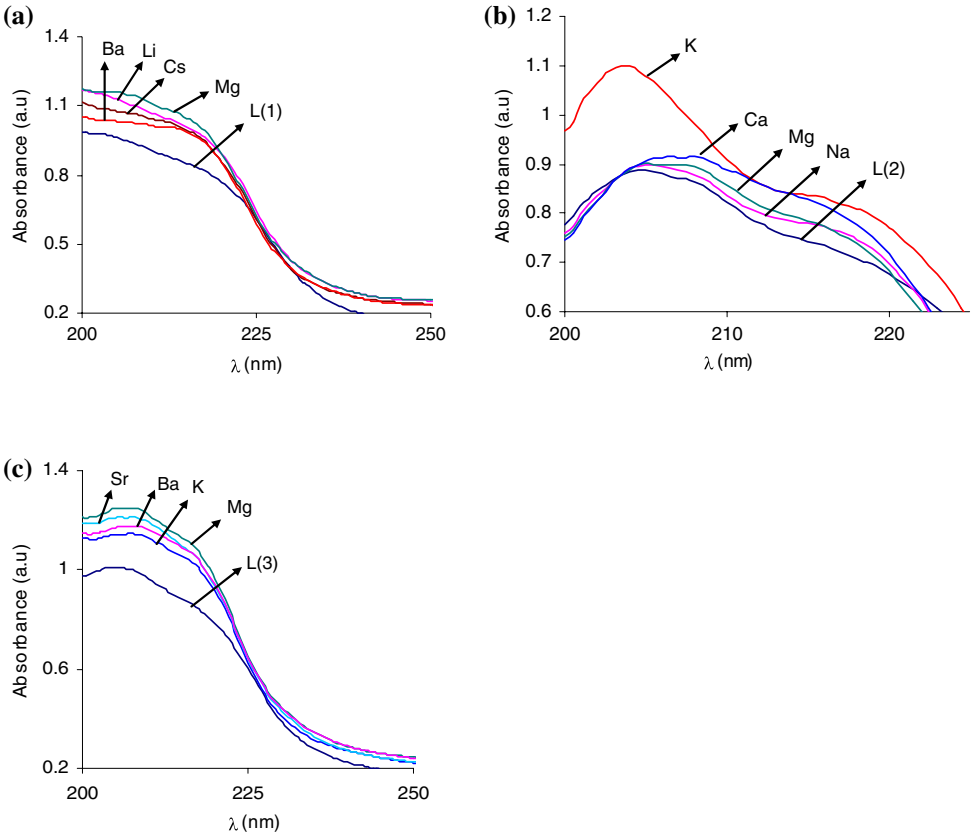

Fig. 2 Absorption spectra of the ionized ligands and their alkali and alkaline earth metal ion complexes in acetonitrile for: (**a**) $(TMA)_2L1$; (**b**) $(TMA)_2L2$; and (**c**) $(TMA)_2L3$

Therefore cation binding results in enhancement of photoinduced charge transfer from the dimethyamine group to the carbonyl group. Consequently, a red shift is observed in the absorption spectra.

As can be seen from the data in Table 1, alkaline earth metal cations cause larger red shifts for the 326 and 328 nm absorption bands than alkali metal cations. The largest red shifts are observed for $(TMA)_2L2$. The larger red shifts for alkaline earth metal cations result from their higher charge density. A similar result for naphthalenic fluorophores is reported in the literature [10].

The introduction of *tert*-butyl groups onto the upper rim of the ligand influences the absorption spectra in the presence of transition metal cations and Pb^{2+}. With the absence *tert*-butyl groups in $(TMA)_2L1$, Fe^{2+}, Fe^{3+} and Hg^{2+} cause blue shifts of 5 nm for the absorption at 326 nm. The other transition metal cations and Pb^{2+} shift the 326 nm absorption band to longer wavelengths. For $(TMA)_2L2$ with two *tert*-butyl groups on the upper rim, Fe^{2+}, Fe^{3+} and Hg^{2+} produce red shifts of 23, 24 and 9 nm, respectively. On the other hand, interaction of Pb^{2+} with $(TMA)_2L2$ causes an 8 nm blue shift. As seen from the data in Table 1, interaction of Pb^{2+} with $(TMA)_2L1$ causes a red shift of 12 nm in the 326 nm absorption band. For $(TMA)_2L3$ with four *tert*-butyl groups on the upper rim, Fe^{3+} and Hg^{2+} cause blue shifts of 7 and 9 nm, respectively. Ag^{+}, Cd^{2+}, Co^{2+}, Mn^{2+} and Zn^{2+} produce only red shifts in the absorptions for all three ligands. $(TMA)_2L2$ has the largest red shifts of the 326 nm band for all of the transition metal cations and Pb^{2+}. A blue shift upon complexation of Pb^{2+} by a calix[4]arene carrying four dansyl groups has been reported in the literature [13].

$(TMA)_2L2$ possesses the second absorption band with a maximum at 252 nm. Effects of metal cations on this band are also recorded in Table 1. All of the metal cations investigated cause red shifts of 2–32 nm. The largest red shift is noted for Pb^{2+}.

The last column in Table 1 shows new absorption bands which appear in the presence of the metal cations with the ionized ligands. Interaction of Pb^{2+} with $(TMA)_2L2$ produces a new band at 217 nm. Interaction of Hg^{2+} with $(TMA)_2L2$ causes a new band at 290 nm with a molar absorption coefficient of 8.0×10^3 cm^{-1} M^{-1}. Interaction of Fe^{3+} with $(TMA)_2L1$ and $(TMA)_2L3$ causes new bands at 277 and 268 nm, respectively. With $(TMA)_2L1$, Ag^{+}, Hg^{2+} and Pb^{2+} produce new bands at 251, 220 and 213 nm, respectively. This indicates strong interactions between the Ag^{+}, Hg^{2+}, Pb^{2+} and Fe^{3+} and $(TMA)_2L1$.

Figure 3 shows the red shifts of the ligand absorptions in the long wavelength band as a function of the metal ion diameter. A good correlation is noted for the earth alkaline metal cations. Thus, Mg^{2+} with the smallest ionic diameter

Table 1 Shifts (nm) and new bands in the absorption spectra of dionized ligands $(TMA)_2$L1-$(TMA)_2$L3 in acetonitrile produced by metal ions

Metal ion	Blue shifts[a] (nm)			Red shifts[a] (nm)			Red shifts[b] (nm)	New bands (nm)		
	L(1)[c]	L(2)[d]	L(3)[e]	L(1)[c]	L(2)[d]	L(3)[e]	L(2)[d]	L(1)[c]	L(2)[d]	L(3)[e]
Li^+	–	–	–	5	8	3	2	–	–	–
Na^+	–	–	–	5	6	3	2	–	–	–
K^+	–	–	–	5	5	3	2	–	–	–
Rb^+	–	–	–	5	5	3	2	–	–	–
Cs^+	–	–	–	5	5	3	2	–	–	–
Mg^{2+}	–	–	–	14	19	11	4	–	–	–
Ca^{2+}	–	–	–	12	14	10	3	–	–	–
Sr^{2+}	–	–	–	10	11	7	2	–	–	–
Ba^{2+}	–	–	–	9	10	5	2	–	–	–
Mn^{2+}	–	–	–	11	16	8	3	–	–	–
Fe^{2+}	5	–	–	–	23	7	2	–	–	–
Fe^{3+}	5	–	7	–	24	–	15	277		268
Co^{2+}	–	–	–	14	16	9	3	–	–	–
Zn^{2+}	–	–	–	15	18	10	4	–	–	–
Ag^+	–	–	–	16	23	8	7	251	–	–
Cd^{2+}	–	–	–	9	12	8	2	–	–	–
Hg^{2+}	5	–	9	–	9	–	2	220	290	–
Pb^{2+}	–	8	–	12	–	7	32	213	217	–

[a] λ_{max} = 326 nm for $(TMA)_2$L1 and $(TMA)_2$L2 and λ_{max} = 328 nm for $(TMA)_2$L3. [b] λ_{max} = 252 nm for $(TMA)_2$L2. [c] L(1) = $(TMA)_2$L1. [d] L(2) = $(TMA)_2$L2. [e] L(3) = $(TMA)_2$L3

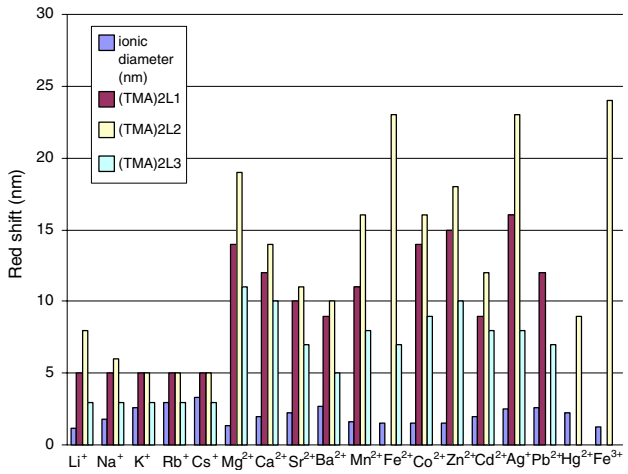

Fig. 3 Bar chart of the red shift of the ionized ligand absorption upon change of metal ion diameter observed at 326 nm for $(TMA)_2$L1 and $(TMA)_2$L2 and at 328 nm for $(TMA)_2$L3

shows the largest red shifts for $(TMA)_2$L1, $(TMA)_2$L2 and $(TMA)_2$L3. The smallest red shifts are observed with Ba^{2+}. $(TMA)_2$L2 exhibits the largest red shifts for all earth alkaline metal cations among the three ligands. For the alkali metal cations, only $(TMA)_2$L2 shows any difference in red shifts as the metal ion is varied. An appreciably larger red shift is noted for Li^+, which has the smallest ionic diameter. For the transition metal ions, no relationship is evident between the magnitudes of the red shifts and metal ion diameters. For Ag^+, Cd^{2+}, Co^{2+}, Mn^{2+} and Zn^{2+}, the magnitudes of the red shifts decrease in the order $(TMA)_2$L2 > $(TMA)_2$L1 > $(TMA)_2$L3. Interestingly, $(TMA)_2$L2 shows the largest red shifts with all the metal ions examined except with Pb^{2+}.

Figure 4 presents the molar absorption coefficients for the long wavelength absorption bands for the three ligands as the metal ion is changed. No pronounced trends are evident as the number of *tert*-butyl groups on the upper rim of the ligand and the identity of the metal ion are varied.

Fluorescence spectra

The fluoroionophoric ligands $(TMA)_2$L1 and $(TMA)_2$L2, when excited at 326 nm, give an emission band with a maximum at 471 nm. When $(TMA)_2$L3 was excited at 328 nm, an emission band with a maximum at 473 nm was observed. Figure 5 shows the effects of metal cations on the fluorescence spectra of $(TMA)_2$L2. As can be seen, the emission band intensities for $(TMA)_2$L2 are reduced somewhat by the presence of alkali metal cations and are diminished substantially for interactions with alkaline earth metal cations. Concomitant are dramatic red shifts of the emission band when Li^+, Na^+, K^+, Rb^+, Cs^+, Mg^{2+}, Ca^{2+}, Sr^{2+} and Ba^{2+} are present. There is strong quenching of the fluorescence emission with the transition metal cations of Ag^+, Cd^{2+}, Co^{2+}, Fe^{2+}, Mn^{2+} and Zn^{2+}. Even

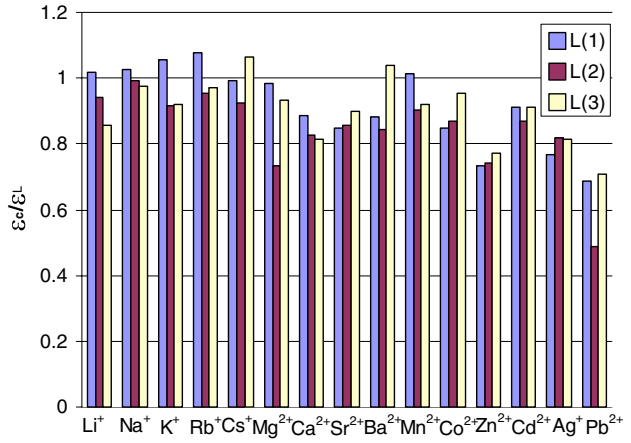

Fig. 4 Bar chart of the ratio of molar absorption coefficients of the metal ion complexes (ε_c) to that of the ionized ligands (ε_l) measured at 326 nm for $(TMA)_2L1$ and $(TMA)_2L2$ and at 328 nm for $(TMA)_2L3$

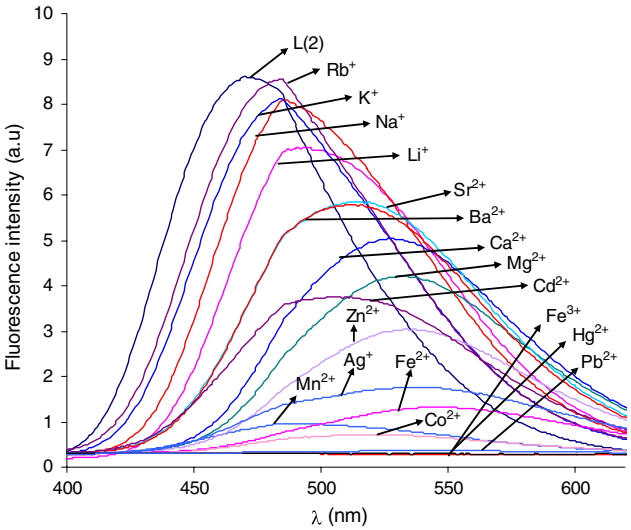

Fig. 5 Effects of metal cations on fluorescence spectra of $(TMA)_2L2$ in acetonitrile. (Ligand concentration = 2.58×10^{-5} M. Monovalent metal perchlorate concentrations = 2.58×10^{-3} M. Divalent metal perchlorate concentration = 1.29×10^{-3} M. Excitation at 326 nm)

stronger quenching is observed with Hg^{2+}, Pb^{2+} and Fe^{3+}. A decrease of the fluorescence intensity caused by Hg^{2+} and Pb^{2+} ions is probably a result of the "heavy atom effect" [21]. The complexation of Fe^{3+} may cause the fluorescence to be quenched via electron or energy transfer to the metal ion, that leads to rapid non-radiative decay.

Figure 6 shows the relationship between the magnitude of the red shifts of the fluorescence emission and the metal ion diameters for the three ligands. There is a good correlation between the magnitude of the red shifts and the alkaline earth metal cation diameters for $(TMA)_2L1$ and$(TMA)_2L2$. Thus decreasing the ionic diameter causes a

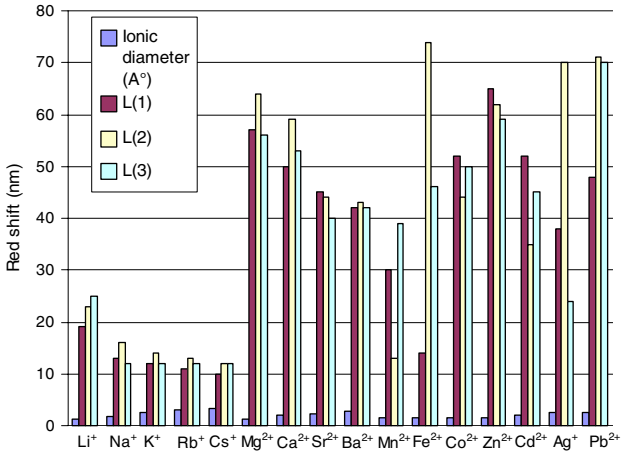

Fig. 6 Bar chart of the red shift of the fluorescence emission observed at 471 nm for $(TMA)_2L1$ and $(TMA)_2L2$ and 473 nm for $(TMA)_2L3$ as a function of the metal ion diameter

greater red shift. All three ligands show the largest red shifts for Li^+ among the alkali metal cations and for Mg^{2+} among the earth alkaline metal cations.

The number of *tert*-butyl groups on the upper rims of the ligands significantly affects the values of red shifts produced by Ag^+, Fe^{2+} and Mn^{2+}. For Mn^{2+}, $(TMA)_2L3$ exhibits the largest red shift of 39 nm. With $(TMA)_2L1$ the red shift for Mn^{2+} decreases to 30 nm and with $(TMA)_2L2$ it plummets to 13 nm. On the other hand for Fe^{2+}, $(TMA)_2L2$ shows the largest red shift of 75 nm among the investigated metal ions. For Cd^{2+}, Co^{2+} and Zn^{2+}, the largest red shifts are noted with $(TMA)_2L1$. For Ag^+, $(TMA)_2L2$ shows a 70 nm red shift which is much larger than those for the other two ligands. Also, Pb^{2+} produces large red shifts, especially for $(TMA)_2L2$ and $(TMA)_2L3$.

Figure 7 shows the fluorescence quenching efficiency for the three ionized ligands upon addition of mono- and

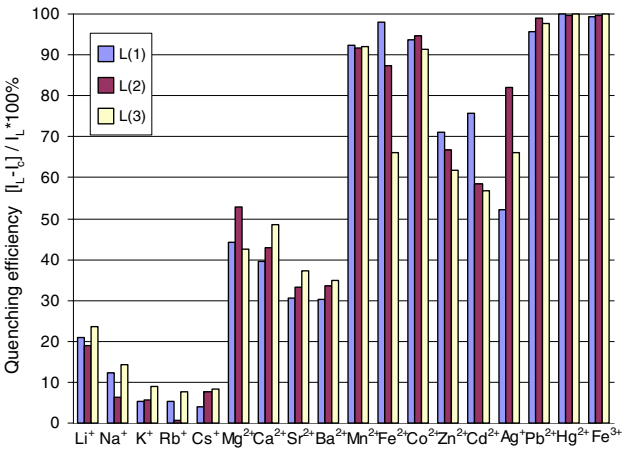

Fig. 7 Bar chart of quenching efficiency for different metal ions observed at 471 nm for $(TMA)_2L1$ and $(TMA)_2L2$ and at 473 nm for $(TMA)_2L3$

di-valent metal ions observed at 471 nm for $(TMA)_2L1$ and $(TMA)_2L2$ and at 473 nm for $(TMA)_2L3$. The transition metal cations and Pb^{2+} produce stronger fluorescence quenching for all three ligands than do the alkali and earth alkaline metal cations. Hg^{2+} and Fe^{3+} give greater than 99% quenching of the fluorescence for all three ligands. The data in Fig. 6 show greater than 90% quenching with all three ligands for Co^{2+}, Mn^{2+} and Pb^{2+}. With Fe^{2+}, there is a pronounced effect of ligand structure on the level of quenching. With the absence of *tert*-butyl groups on the upper rim of $(TMA)_2L1$, there is 98% fluorescence quenching. The presence of two and then four *tert*-butyl groups in the ligand substantially decreases the extent of fluorescence quenching by Fe^{2+}.

Determination of stability constants

The stability constants and the stoichiometry for complexation of Hg^{2+}, Pb^{2+} and Fe^{3+} with the three ligands was determined by fluorimetric titration. The titration experiments were performed by adding solutions with various concentrations of metal perchlorate in acetonitrile to solutions of the ionized ligand in the same solvent. The ligand concentration was held constant at 2.58×10^{-5} M. The stoichiometries of the complexes and their stability constants were determined from changes in the fluorescence intensity as a function of the cation concentration. Successive decreases of emission with increases of the metal ion concentration eventually caused a complete disappearance of the emission in all of the fluorimetric titrations.

Figure 8 shows the fluorescence spectra of $(TMA)_2L3$ in acetonitrile with increasing concentrations of Pb^{2+}. The insert in Fig. 8 is a plot of the fluorescence intensity versus the ratio of [metal ion]/[ligand]. The break in the curve at

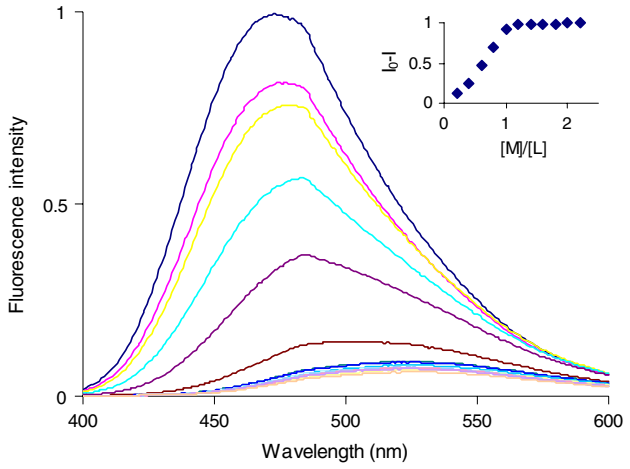

Fig. 8 Fluorescence spectra ($\lambda_{exc} = 328$ nm) of $(TMA)_2L3$ (2.58×10^{-5} M) in acetonitrile with increasing concentrations of Pb^{2+}

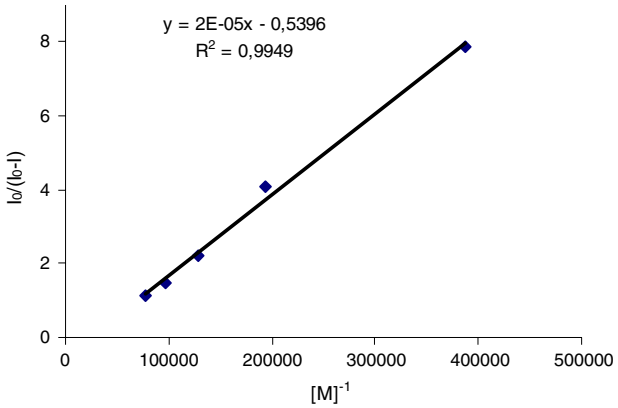

Fig. 9 Plot of $I_o/(I_o-I)$ versus $[Pb^{2+}]^{-1}$ for the spectrofluorimetric titration of $(TMA)_2L3$ (2.58×10^{-5} M) with Pb^{2+} in acetonitrile

Table 2 Stability constants for complexes of ionized calixarenes $(TMA)_2L1$-$(TMA)_2L3$ with Hg^{2+}, Pb^{2+} and Fe^{3+} in acetonitrile

Stability constant (log β)			
Ionized ligand	Cation		
	Fe^{3+}	Hg^{2+}	Pb^{2+}
$(TMA)_2L1$	3.94 ± 0.02	4.53 ± 0.03	4.76 ± 0.04
$(TMA)_2L2$	4.74 ± 0.04	4.83 ± 0.03	4.26 ± 0.03
$(TMA)_2L3$	4.06 ± 0.03	3.84 ± 0.02	4.43 ± 0.02

[metal ion]/[ligand] = 1.0 provides strong evidence for formation of a 1:1 complex. Similar plots are found for all three ligands with Hg^{2+}, Pb^{2+} and Fe^{3+} in acetonitrile.

The complex stability constant (β) was calculated using Valuer's method [19]. Accordingly the quantity $I_o/(I_o-I)$ is plotted versus $[\text{metal ion}]^{-1}$ with the stability constant given by the ratio of intercept/slope. Figure 9, a plot of $I_o/(I_o-I)$ versus $[Pb^{2+}]^{-1}$ for $(TMA)_2L3$, which shows satisfactory linearity.

Table 2 presents calculated stability constants for complexation of $(TMA)_2L1$, $(TMA)_2L2$ and $(TMA)_2L3$ with Fe^{3+}, Hg^{2+} and Pb^{2+}. The log β values of 3.8–4.8 demonstrate strong interactions of these metal ions with the ionized ligands in acetonitrile. For Fe^{3+} and Hg^{2+}, $(TMA)_2L2$ has the largest stability constant. On the other hand, (TMA)L2 is the weakest ligand for Pb^{2+} and (TMA)L1 is the strongest. Thus the data presented in Table 2 do not allow one to discern the influence of *tert*-butyl groups on the upper rims of these ligands upon the strength of transition metal ion complexation.

Acknowledgments This work was supported by The Scientific and Technological Research Council of Turkey (TUBITAK). We also thank the Division of Chemical Sciences, Geosciences and Biosciences of the Office of Basic Energy Sciences of the US Department of Energy (Grant DE-FG02-90ER14416) for support of this research.

References

1. Gutsche, C.D.: Calixarenes. Royal Society of Chemistry, Cambridge, England (1989)
2. Vicens, J., Böhmer, V. (eds.): Calixarenes: A Versatile Class of Macrocyclic Compounds. Kluwer Academic Publishers, London (1991)
3. Gutsche, C.D.: Calixarenes Revisited. Royal Society of Chemistry, Cambridge, England (1998)
4. Beer, P.D., Gale, P.A., Smith, D.K.: Citation binding. In: Evans, J. (ed.) Supramolecular Chemistry. Oxford University Press, New York (1999)
5. Mandolini, L., Ungaro, R. (eds.): Calixarenes in Action. Imperial College Press, London (2000)
6. Asfari, Z., Böhmer, V., Harrowfield, J., Vicens, J. (eds.): Calixarenes 2001. Kluwer Academic Publishers, London (2001)
7. Kim, J.S., Quang, D.T.: Calixarene-derived fluorescent probes. Chem. Rev. **107**, 3780–3799 (2007). doi:10.1021/cr068046j
8. Iwamoto, K., Araki, K., Fujishima, H., Shinkai, S.: Fluoregenic calix[4]arene. J. Chem. Soc. Perkin Trans. **1**, 1885–1887 (1992). doi:10.1039/p19920001885
9. Ji, H.F., Yang, Y., Xu, X., Brown, G.: A calixarene based fluorescent Sr^{2+} and Ca^{2+}. Org. Biomol. Chem. **4**, 770–772 (2006). doi:10.1039/b517877k
10. Leray, I., O'Reilly, F., Habib Jiwan, J.-L., Soumillion, J.-Ph., Valuer, B.: A new calixarene[4]-based fluorescent sensor for sodium ion. Chem. Commun. (Camb.) 795–796 (1999) doi:10.1039/a900020h
11. Narita, M., Higuchi, Y., Hamada, F., Kumagai, H.: Metal sensor of water soluble dansyl-modified thiacalix[4]arenes. Tetrahedron Lett. **39**, 8687–8690 (1998). doi:10.1016/S0040-4039(98)01899-1
12. Narita, M., Hamada, F., Sato, M., Suzuki, I., Osa, T.: Fluorescent molecular recognation and sensing system of bis-dansyl modified γ-cyclodextrins. J. Inclusion Phenom **34**, 421–430 (1999). doi:10.1023/A:1008086700570
13. Metivier, R., Leray, I., Valeur, B.: A highly sensitive and selective fluorescent molecular sensor for Pb(II) based an a calix[4]arene bearing four dansyl groups. Chem. Commun. (Camb.) 996–997 (2003) doi:10.1039/b301323e
14. Chen, Q.Y., Chen, C.F.: A new Hg^{2+}-selective fluorescent sensor based on a dansyl amide-armed calix[4]-aza-crown. Tetrahedron Lett. **46**, 165–168 (2005). doi:10.1016/j.tetlet.2004.10.169
15. Talanova, G.G., Elkarim, N.S.A., Talanov, V.S., Bartsch, R.A.: A calixarene-based fluoregenic reagent for selective mercury (II) recognation. Anal. Chem. **71**, 3106–3109 (1999). doi:10.1021/ac990205u
16. Talanova, G.G., Roper, E.D., Buie, N.M., Gorbunova, M.G., Bartsch, R.A., Talanov, V.S.: Novel fluorogenic calix[4] arene-bis (crown-6-ether) for selective recognition of thallium(I). Chem. Commun. (Camb.) 5673–5675 (2005) doi:10.1039/b510348g
17. Metivier, R., Leray, I., Valeur, B.: Lead and mercury sensing by calixarene-based fluoroionophores bearing two or four dansyl fluorophores. Chem. Eur. J. **10**, 4480–4490 (2004). doi:10.1002/chem.200400259
18. Metivier, R., Leray, I., Lebeau, B., Valeur, B.: A mesoporous silica functionalized by a covalently bound calixarene-based fluoroionophore for selective optical sensing of mercury(II) in water. J. Mater. Chem. **15**, 2965–2973 (2005). doi:10.1039/b501897h
19. Bourson, J., Valeur, B.: Ion-responsive fluorescent compounds. Cation-steered intramolecular charge transfer in a crowned merocyanine. J. Phys. Chem. **93**, 3871–3876 (1989). doi:10.1021/j100346a099
20. Talanova, G.G., Talanov, V.S., Gorbunova, M.G., Hwang, H.S., Bartsch, R.A.: Effect of upper rim para-alkyl substituents on extraction of alkali and alkaline earth metal cations by di-ionizable calix[4]arenes. J. Chem. Soc. Perkin Trans. **2**, 2072–2077 (2002). doi:10.1039/b207301c
21. Aragoni, M.C., Arca, N., Bencini, A., Blake, A.J., Caltagirone, C., Danesi, A.: New fluorescent chemosensors for heavy metal ions based on functionalized pendant arm derivatives of 7-anthracenylmethyl-1,4,10-trioxa-7,13-diazacyclopentadecane. Inorg. Chem. **46**, 8088–8097 (2007). doi:10.1021/ic700657j